Electronic Supplementary Material (ESI) for Nanoscale.
This journal is © The Royal Society of Chemistry 2023

Supplementary Information for

Accelerating structure reconstruction to form NiOOH in metal-organic frameworks (MOFs) for boosting oxygen evolution reaction

Ruiyao Hou,[b] Xiaoxia Yang,[b] Linghui Su,[d] Wanglai Cen,[de] Lin Ye,[c] Dengrong Sun*[ae]

[a] College of Carbon Neutrality Future Technology, Sichuan University, Chengdu, P. R. China

[b] College of Architecture and Environment, Sichuan University, Chengdu 610065 (China)

[c] College of Materials and Chemistry & Chemical Engineering, Chengdu University of Technology, Chengdu 610059, P. R. China

[d] Institute of New Energy and Low Carbon Technology, Sichuan University, Chengdu, P. R. China

[e] National Engineering Research Centre for Flue Gas Desulfurization, Chengdu, P. R. China

Email: dengrongsun@hotmail.com; dengrongsun@scu.edu.cn (D. Sun)

Experimental Section

Materials $NiCl_2 \cdot 6H_2O$ (98.0%), $Ni(NO_3)_2 \cdot 6H_2O$ (98%), $Fe(NO_3)_3 \cdot 9H_2O$ (98.5%) and KOH (85.0%) were purchased from Chron Chemical Co. 1,4-Benzenedicarboxylic acid (H_2BDC) (98%) and N, N-dimethylformamide (DMF) (99.8%) were purchased from Sigma Aldrich Co. Triethylamine (TEA) (99.0%) and urea (99.5%) were purchased from Aladdin Co. All reagents were used as received without further purifications.

Synthesis of Ni-BDC Ni-BDC was prepared according to the previously reported procedures with slight modifications.[1] Firstly, 32 mL DMF, 2 mL ethanol and 2 mL ultrapure water were mixed in a 100 mL glass bottle. Then, 0.75 mmol H_2BDC and 0.75 mmol $NiCl_2 \cdot 6H_2O$ were added to the above solution and dissolved. After complete dissolution, 0.8 mL TEA was rapidly injected into the solution. The solution was then stirred for 5 min to obtain a uniform colloidal suspension. Afterwards, the solution was ultrasonicated continuously for 8 h (40 kHz) under confine condition. Eventually, the light green precipitate was collected via centrifugation and washed with ethanol and water for three times, respectively, followed by vacuum freeze-drying for over 12 h to obtain the final product.

Synthesis of $NiFe_2O_4$/NiFe LDH $NiFe_2O_4$/NiFe LDH was prepared by a hydrothermal method. 1.5 mmol of $Ni(NO_3)_2 \cdot 6H_2O$, 0.5 mmol of $Fe(NO_3)_3 \cdot 9H_2O$ and 2.5 mmol of urea were added to a 100 ml Teflon-lined stainless steel autoclave containing 35 mL ultrapure water. Then, it was hydrothermally treated at 120 °C for 10 h. After the reaction, the precipitate was obtained by centrifugation and washed with ethanol and water for three times (the last time must be washed with water), respectively, and then vacuum freeze dried for over 12 h.

Synthesis of $NiFe_2O_4$/NiFe LDH@Ni-BDC $NiFe_2O_4$/NiFe LDH@Ni-BDC was prepared under similar condition with that of $NiFe_2O_4$/NiFe LDH. Ni-BDC (52 mg), $Fe(NO_3)_3 \cdot 9H_2O$ (15 mg) and urea (72 mg) were dissolved in a 50 ml Teflon-lined stainless steel autoclave containing 20 mL ethanol and then stirred with a glass rod to form uniform solution. The suspension was then hydrothermally treated at 120 °C for 10 h. After the reaction, the precipitate was obtained by centrifugation and washed with ethanol and water for three times, respectively, and then vacuum freezing dried for over 12 h to finally obtain $NiFe_2O_4$/NiFe LDH@Ni-BDC-4-1. As well, $NiFe_2O_4$/NiFe LDH@Ni-BDC-2-1/1-1/1-2 were prepared by increasing the amount of $Fe(NO_3)_3 \cdot 9H_2O$ and urea in equal proportion. Besides, the comparison sample Ni-BDC-Fe was also prepared in the same way but without urea.

Characterizations X-ray powder diffraction (XRD) patterns were measured on a high-resolution powder X-ray diffractometer (DX-2700) with Cu Kα as the radiation source. The data was collected within the 2θ range of 5-80 degrees. SEM images was taken on FIB-SEM (Thermo Scientific Helios 5CX). Atomic force microscopy (AFM) were recorded using Bruker Dimension Icon (ScanAsyst in Air, 1Hz). X-ray photoelectron spectroscopy (XPS) was performed on Thermo Scientific Nexsa, and all binding energies were calibrated by the C 1s peak at 284.6 eV. FT-IR and *in-situ* FT-IR spectra were scanned with the FT-IR spectrometer (Nicolet iS50FT-IR).

Electrochemical measurements An electrochemical workstation (CHI 760E) with a typical three-electrode system was used to measure the electrochemical performance at room temperature. A Pt wire and an Hg/HgO electrode were used as the counter and reference electrodes, respectively, and the prepared catalyst with an area of 0.4×0.5 cm^2 performed as the working electrode. The method of preparing working electrode by loading catalysts on the carbon paper was referred to previous report.[2] The oxygen evolution reaction (OER) was performed in the O_2-saturated 0.85 M KOH (pH≈13.2) aqueous solution. The linear sweep voltammetry (LSV) curves were recorded at a rate of 5 mV s^{-1} to minimize capacitive current with iR compensation. All potentials in this study shown versus reversible hydrogen electrode (RHE) via the following equations: $E_{RHE} = E_{Hg/HgO} + 0.0592 \times pH + 0.098$ V.

***in-situ* FT-IR measurements** The FT-IR spectrometer (Nicolet iS50FT-IR) equipped with an attenuated total reflectance (ATR) electrolytic cell (ElectroChem IR) and a MCT detector cooled by liquid N_2 was used for *in-situ* FT-IR measurement. The samples were made into homogeneous solution following the above electrochemical steps, and 20 μL of the solution was loaded on the center of a gold-plated silicon crystal as the working electrode. The counter and reference electrodes were Pt wire and Ag/AgCl electrode, respectively. FT-IR spectra was recorded from 0.0 V while performing i-t measurements with increasing intervals of 0.1 V. The potentials in this study were shown versus reversible hydrogen electrode (RHE) via the following equations: $E_{RHE} = E_{Ag/AgCl} + 0.0592 \times pH + 0.197$ V

References:

[1] B. Han, X. Ou, Z. Deng, Y. Song, C. Tian, H. Deng, Y.-J. Xu and Z. Lin, *Angew. Chem. Int. Ed.*, 2018, **57**, 16811-16815.

[2] D. Sun, L. W. Wong, H. Y. Wong, K. H. Lai, L. Ye, X. Xv, T. H. Ly, Q. Deng and J. Zhao, *Angew. Chem. Int. Ed.*, 2023, **62**, e202216008.

Fig. S1 Photographs of Ni-BDC (left), $NiFe_2O_4$/NiFe LDH@Ni-BDC (middle) and $NiFe_2O_4$/NiFe LDH (right).

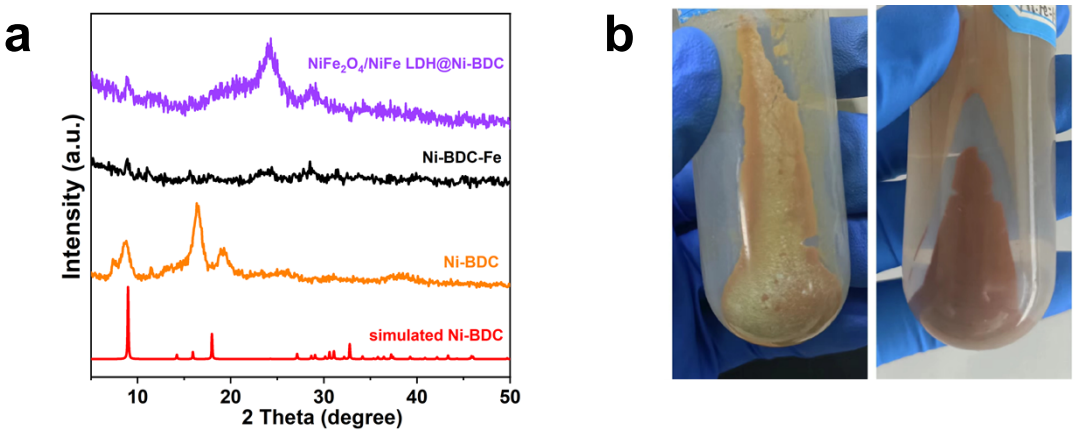

Fig. S2 (a) XRD patterns of Ni-BDC-Fe, $NiFe_2O_4$/NiFe LDH@Ni-BDC, Ni-BDC and simulated Ni-BDC. (b) Photographs of Ni-BDC-Fe (left) and $NiFe_2O_4$/NiFe LDH@Ni-BDC (right).

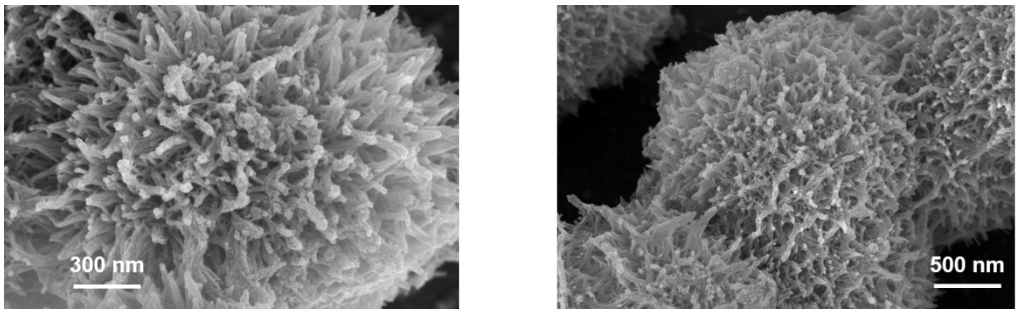

Fig. S3 SEM images of $NiFe_2O_4$/NiFe LDH.

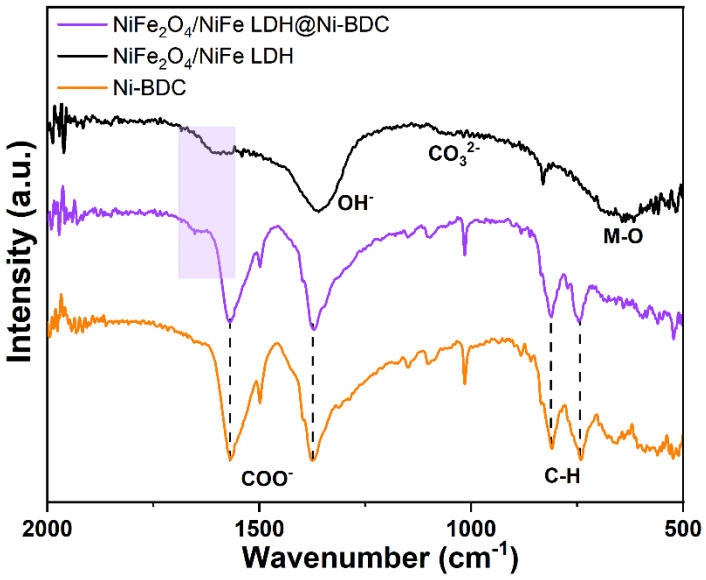

Fig. S4 FT-IR spectra of Ni-BDC, $NiFe_2O_4$/NiFe LDH and $NiFe_2O_4$/NiFe LDH@Ni-BDC.

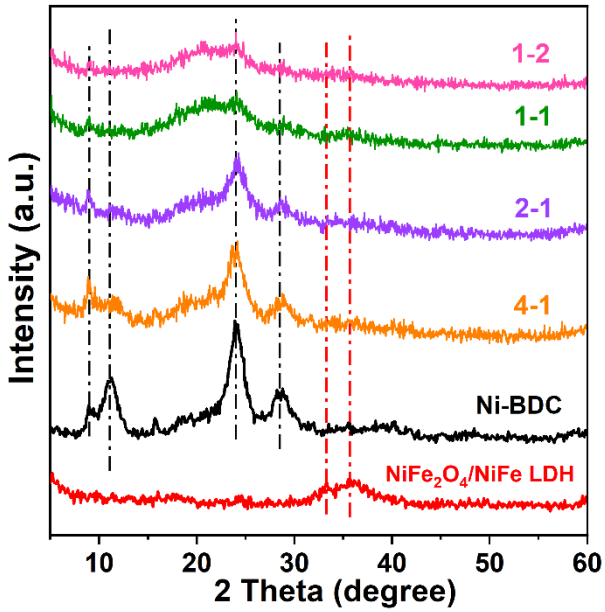

Fig. S5 XRD patterns of $NiFe_2O_4$/NiFe LDH@Ni-BDC of different Ni:Fe feeding ratios, Ni-BDC and $NiFe_2O_4$/NiFe LDH.

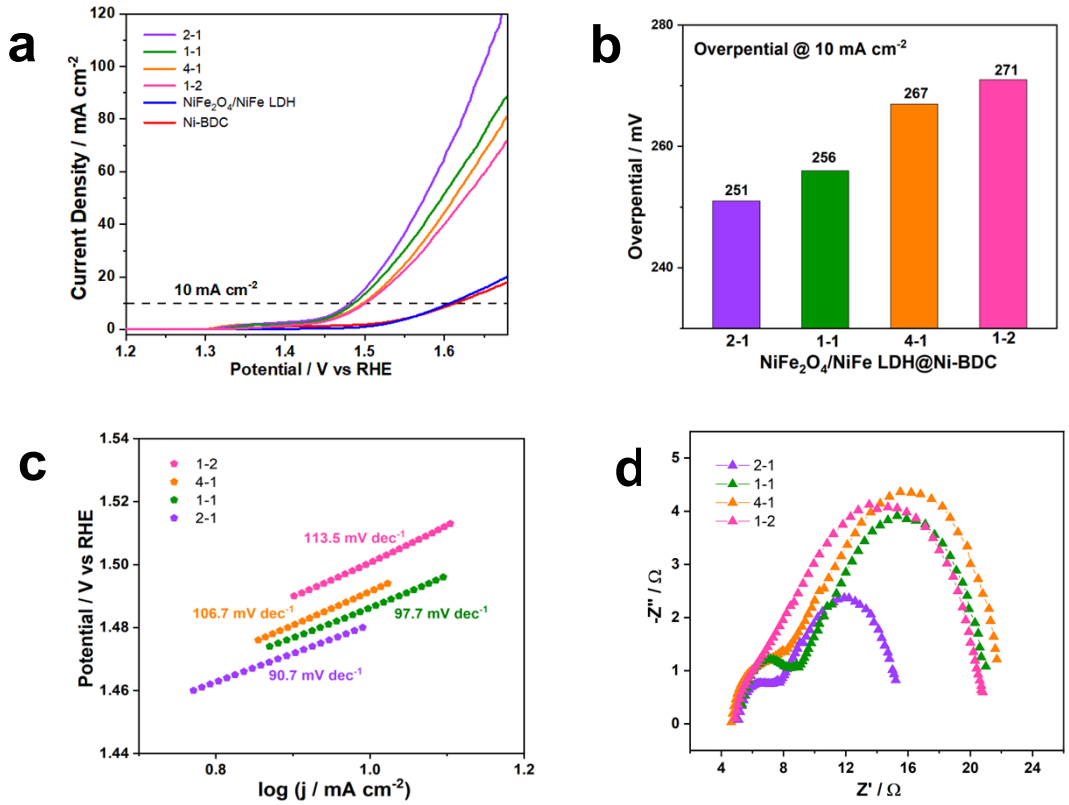

Fig. S6 $NiFe_2O_4$/NiFe LDH@Ni-BDC of different Ni:Fe feeding ratios. (a) LSV curves. (b) Corresponding overpotentials @ 10 mA cm^{-2}. (c) Tafel plots. (d) EIS.

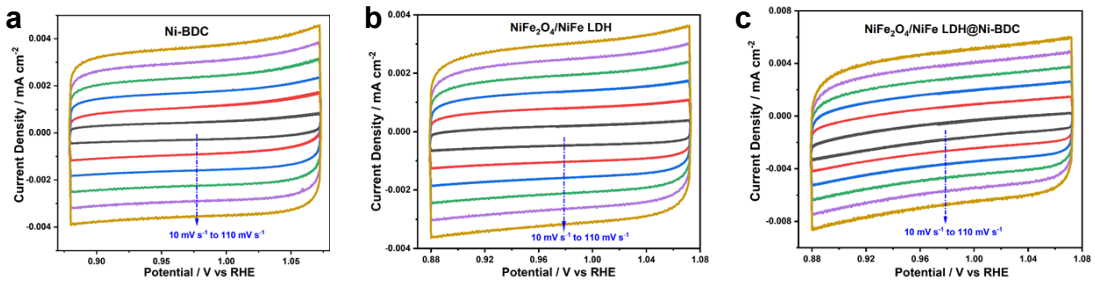

Fig. S7 CV curves of (a) Ni-BDC, (b) $NiFe_2O_4$/NiFe LDH and (c) $NiFe_2O_4$/NiFe LDH@Ni-BDC at different scan rates.

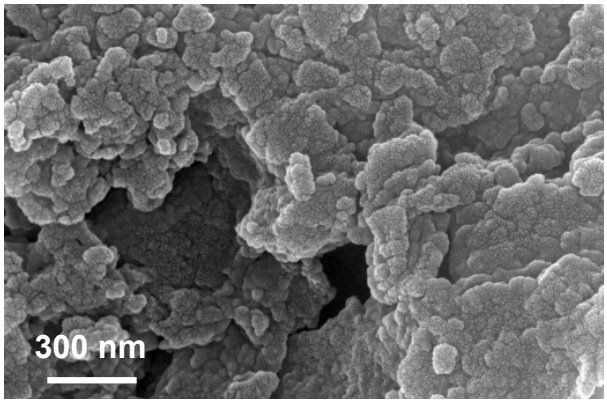

Fig. S8 SEM image of $NiFe_2O_4$/NiFe LDH@Ni-BDC after OER test.

Table S1 Comparison of the OER performance between the $NiFe_2O_4$/NiFe LDH@Ni-BDC and other MOFs-/LDH-based composites reported previously.

Electrocatalyst	Overpotential / mV At 10 mA cm^{-2}	Electrolyte (KOH)	Substrate	Reference
$NiFe_2O_4$/NiFe LDH@Ni-BDC	251	0.85 M	CP	**This work**
NiFe-LDH/$NiCo_2O_4$	290	1 M	NF	ACS Appl. Mater. Interfaces **2017**, 9, 1488-1495
NiFe LDH@NiCoP	220	1 M	NF	Adv. Funct. Mater. **2018**, 28, 1706847
NiFeCo-LDH/CF	249	1 M	GC	Small **2020**, 16, 2002426
Co@NiFe-LDH	253	1 M	RDE	Mater. Chem. A **2022**, 10, 5244-5254
Ni-MOF/NiFe-MOF	296/240	0.1 M	NF	Nat. Commun. **2017**, 8, 15341
Ni-MOF@Fe-MOF	256	1 M	GC	Adv. Funct. Mater **2017**, 27, 1702546
Ni-MOF/Co-MOF	355/394	1 M	GC	New J. Chem. **2022**, 46, 18996-19001
Fe_1Ni_2-BDC	260	1 M	GC	ACS Energy Lett. **2019**, 4, 285-292
Ni-BDC-1R	225	1 M	NF	Angew. Chem. Int. Ed. **2022**, 61, e202214794
Fe-MOFs@Ni-MOFs	275	1 M	CP	Small **2019**, 15, 1903410
β-$Ni(OH)_2$/Ni-MOF	263	1 M	NF	Inorg. Chem. **2020**, 59, 4764-4771
Co_3O_4@Co-MOF	277	1 M	GC	Chem. Commun. **2019**, 55, 10904-10907
$Fe(OH)_3$@Co-MOF-74	292	1 M	CP	ChemSusChem **2019**, 12, 4623-4628